

改善低溫複晶矽薄膜電晶體均勻性之元件結構 與校正電路之研究

研究生：陳柏廷

指導教授：鄭晃忠 博士

戴亞翔 博士

國立交通大學電子工程學系暨電子研究所博士班

摘要

在本篇論文當中，我們運用低溫複晶矽薄膜電晶體為元件，分別從元件結構以及其顯示器應用電路設計兩方面來探討均勻性之問題。在此研究中，我們藉由佈局方式簡單地調整元件架構來提升低溫複晶矽薄膜電晶體之均勻性，此外亦提出對元件變異性具有高度補償能力之主動矩陣式有機發光二極體畫素電路以及源極隨耦器形式的類比緩衝電路。

首先，我們從元件結構之觀點來探討低溫複晶矽薄膜電晶體之元件均勻性。我們採用了交叉以及多通道之元件佈局。根據實驗之結果，我們發現交叉方式佈局可以提升相鄰電晶體之均勻性，而多通道結構可以提升低溫複晶矽薄膜電晶體整體之截止電壓及次臨界擺幅之均勻性。針對此結果，我們也進一步進行機制之探討，認為晶粒機率分佈之現象是致使均勻性提升最主要之原因。

在主動矩陣式有機發光二極體畫素電路當中，我們針對各個電晶體尺寸及電容大小進行探討。傳統的畫素架構，經由實際量測結果，可以很清楚的瞭解當驅動電晶體的截止電壓有所不同時，有機發光二極體陽極電壓也會有明顯之差異，因此畫素彼此之間輸出電流有所差異，而導致畫面亮度之不均勻。相較於傳統佈

局的方式，運用前述提出之多通道之結構佈局除了可以有效增大電流，亦可獲得畫素陽極電壓均勻性較佳之結果。

我們先提出一種新型的電路操作模式來校正低溫複晶矽薄膜電晶體之截止電壓變異性之問題。藉由實際量測結果證實，我們所提出的電路架構確實可以有效地縮小輸出電壓變異性之問題，而且可以獲得輸出電壓增大的好處。然而，在重置階段時有機發光二極體亦會有電流通過，而導致整體畫素電路消耗功率將因而提升。因此，我們進一步提出第二種電路操作模式來改善上述的缺點。我們將其中一個電晶體由 N 型換成 P 型，並改由切換訊號控制，在重置階段時此電晶體將阻止不必要的電流流過有機發光二極體，藉以降低整體消耗功率。

在類比緩衝電路設計之研究中，我們了解在液晶顯示器源極驅動器內的類比緩衝器在整合至玻璃基板時，元件的變異性亦極有可能導致實際輸出電壓與目標電壓有所差異。因此，我們亦將多通道結構引入傳統驅動架構中，藉由觀察類比緩衝電路之輸出特性再次驗證多通道結構對薄膜電晶體均勻性提升之能力。由量測結果可以得知具有多通道結構之源極隨耦器形式的類比緩衝電路，其輸出電壓之變異性有明顯地降低，證實多通道結構不論對於前述之畫素電路或是類比緩衝器電路之均勻性均具有明顯改善。如同畫素電路，傳統之類比換衝器無法達到規格需求，因此採用校正電路是必要的。文獻上各種已報導之類比緩衝器電路亦會做整理，在比較各種表現之後，我們認為源極隨耦器形式是較佳之選擇。

傳統的低溫複晶矽薄膜電晶體源極隨耦器具有一個驅動的電晶體，可以明顯的從模擬結果當中得知，輸出電壓並不是固定在預期的輸入電壓減去臨界電壓值，而是呈現一個不飽和的緩步上升現象，我們認為這是因為低溫複晶矽薄膜電晶體的次臨界電流持續在充電之緣故。因此，我們在傳統源極隨耦器加一主動式負載藉以消除輸出電壓的不飽和現象，加了主動式負載後的輸出電壓偏移量與充電時間並無相依性，雖然其偏移量較大，但可藉由灰階校正去補償，所以我們可以得知加上主動式負載後的傳統源極隨耦器對於設計者而言有較佳的助益。

但即使消除了輸出電壓不飽和現象，元件的變異性問題卻依然存在。因此我

們提出一種校正電路，藉以解決變異性過大的問題，此電路包含了四個開關、一個儲存電容以及兩個低溫複晶矽薄膜電晶體。藉由此操作，輸出電壓端的電壓值相當近似輸入電壓值。此外，我們亦發現主動式負載之閘極偏壓對電路輸出偏差具有顯著的影響，可藉由適當的偏壓設計達到具高度均勻性、良好輸出特性以及低功率消耗之類比緩衝電路。



Study on the Uniformity Improvement of Low-Temperature Polycrystalline-Silicon Thin Film Transistors with the Device Structures and Compensated Circuits

Student: Bo-Ting Chen

Advisor: Dr. Huang-Chung Cheng
Dr. Ya-Hsiang Tai

Department of Electronics Engineering & Institute of Electronics
College of Electrical Engineering and Computer Science
National Chiao Tung University



ABSTRACT

The uniformity issues of the low-temperature polycrystalline silicon thin film transistors (LTPS TFTs) were investigated from the individual aspects of device structure and the display driving circuits design in this dissertation. In this work, the device structure is adjusted to improve the uniformity of LTPS TFTs by changing layout method. Furthermore, active matrix organic light emitting diode pixel circuits and a source follower type analog buffer circuit with highly compensating capability are also proposed.

First of all, the device uniformity of LTPS TFTs is studied from the view point of device structure. The interdigitated and multi-channel structure with slicing layout

method is adopted in this work. According to the experimental results, it is observed that the interdigitated layout the multi-channel structure can promote the matched transistors and overall uniformity of threshold voltage and subthreshold swing of LTPS TFTs. The possible mechanisms of the improving uniformity of multi-channel structure are discussed and it is considered that probability effect is the most major reason.

In the active matrix organic light emitting diode (OLED) pixel design, each function of transistors and capacitor are investigated. Through the measured results in the typical pixel circuits, there is clear difference existing in OLED anode voltage when the threshold voltages of driving transistors are varied. Therefore, the output currents are varied from pixel to pixel leading the non-uniform brightness. Compared with conventional layout method, the multi-channel structure with slicing layout of driving TFT in previous work can enhance the output current and promote uniformity of the pixel anode voltage effectively.

A pixel circuit with new operation mode is proposed to compensate the variation of threshold voltage in LTPS TFTs. By means of experimental results, it is verified that the proposed pixel circuit can solve the problem of output voltage variation effectively and higher output voltage can be obtained. However, the power consumption is increased because current flow through OLED device in the reset period. Therefore, a modified circuit design is further proposed to overcome the issue. By modifying pixel design, an n channel TFT is replaced by a p channel TFT controlled by the switching signal in order to block the current flow through OLED during pre-charge period and the overall power consumption can be lowered.

In the analog buffer circuit, the device variations may lead to the difference between input voltage and output voltage when the analog buffer is applied to the

source driver of liquid crystal displays or integrated into glass substrate. Meanwhile, the output variations of the conventional source follower with multi-channel structure are also introduced. It can be observed that the output variations are apparently reduced comparing with conventional source follower. It is proved that the uniformity of previous pixel circuit or analog buffer circuit can be improved by multi-channel structure. The traditional analog buffer circuit can not achieve the specific requirement like the one of pixel circuit. Therefore, the compensation circuit for analog buffer is necessary. In this dissertation, all kinds of analog buffer circuits are introduced and compared, while the source follower type is considered as the better choice.

The conventional source follower consists of one driving transistor. It is observed from the simulation results that the final output voltage is not kept constant, but exceeds the value of $V_{gs} - V_{th}$ expected in principle. It is ascribed to the sub-threshold current which charges the circuit continuously. As a result, it will be sensitive to the charging time for various product specifications. Therefore, an active load is added to eliminate this unsaturated phenomenon of the output voltage and the deviation of output voltage has no relation to the charging time. Although this offset voltage deviation is larger, it can be compensated by external gamma correction. Therefore, the conventional source follower with an active load has better performance for the designers.

Nevertheless, the simulation results show that the circuit suffers from huge variations and output voltage is not the same due to the variations of TFTs even eliminating the output voltage unsaturated phenomenon. Therefore, a new analog buffer which consists of four switches, a capacitor, and two LTPS TFTs is proposed for the compensation of the device variation. The operating principles are described as follows. The output voltage is compensated by the voltage stored in C_{vt} and almost

equals to input voltage. Besides, the bias voltage of an active load has great influence on output voltage deviation. By means of proper bias voltage design, a highly uniformed, excellent output characteristic and low power consumption analog buffer circuit can be obtained.



誌 謝

僅以此論文獻給我最敬愛的父母-陳澤敏先生與王婉津女士，感謝你們多年來辛苦的養育我，教導我，有了你們持續的支持與付出，讓我得以全心全意投入學業無後顧之憂，順利完成博士學位，同時也要感謝我的弟弟-陳建銘先生，在生活上互相的砥礪扶持及幫忙。

感謝我的論文指導教授鄭晃忠博士以及戴亞翔博士，老師們在研究上的不遺餘力地教導以及生活上的待人處事，都使我獲益良多，也幫助我能順利完成學業，獲得博士學位。感謝我的論文口試委員，有了委員們的熱心建議與指導，使論文能更趨於完整。

感謝實驗室的學長、同學及學弟們，謝謝你們不管在實驗或是生活上都能夠給予我支持與關心，使得我的研究能夠順利完成，其中包含了曾章和學長、林敬偉學長、陳國基學長、阮全平學長、常鼎國學長、張原熏學長、朱芳村學長、曾懷遠學長、詹爵魁學長、郭孟維學長、林高照學長、蔡春乾學長、張國瑞學長、賴瑞霖同學、郭育如學妹、江可玉學妹、莊宗穎學弟、廖大傳學弟、張耀仁學弟、魏瑛君學妹、陳旭信學弟、許鈞凱學弟、邵瀚忠學弟、韋凱方學弟、林心瑜學妹、王祐圻學弟、張佩琪學妹以及陳俠威學弟，有了你們的相伴與合作此論文才能順利完成。

同時感謝國立交通大學奈米中心及國家奈米元件實驗室提供最優良的設備與研究環境，也感謝何唯梅小姐、劉曉玲小姐於行政事務上之幫忙，感謝工業技術研究院以及中華映管股份有限公司等，在製程上的大力協助及幫忙。

最後感謝所有曾經幫助過我的親朋好友們，謝謝你們一路上給我的支持與關心，我今天才可以完成博士學位，謝謝大家。

Contents

Abstract (in Chinese)	i
Abstract (in English)	iv
Acknowledgments (in Chinese)	viii
Contents	ix
Table Lists	xv
Figure Captions	xvi

Chapter 1 Introduction.....1

1.1 Overview of Low-Temperature Polycrystalline-Silicon Thin-Film Transistors (LTPS TFT) Technology.....	1
1.2 Overview of the Organic Light Emitting Diode (OLED) Displays.....	5
1.2.1 Passive Matrix OLED and Active Matrix OLED.....	6
1.2.2 Emission Structures for AMOLED.....	7
1.2.3 Driving Architecture Comparison between AMLCD and AMOLED...10	
1.2.4 Comparison of Transistor Types: A-Si TFTs vs. LTPS TFTs.....	11
1.3 System on a Panel (SOP) Issues and Concept in LTPS TFTs.....	12
1.3.1 Concept of System on a Panel.....	13
1.3.2 Peripheral Circuitries across the Panel.....	14
1.3.3 Critical Issues of System on Panel.....	15
1.4 Motivation.....	18
1.4.1 From the Aspect of Device Structures – Interdigitated Layout and Multi-channel Structure to Improve Uniformity between LTPS-TFTs.....	19
1.4.2 From the Aspect of Circuit Design -- Pixel Compensation Circuits for AMOLEDs and Source Follower Type Analog Buffers for System on Panel...19	

1.5 Dissertation Organization.....	20
Chapter 2 Uniformity in the Interdigitated Layout and Multi-channel Structure of Low-Temperature Polycrystalline Silicon Thin Film Transistors	23
2.1 Introduction.....	23
2.2 Dimensional Effects and Layout Methods on the Matching Properties of P-channel Low-Temperature Polycrystalline Silicon Thin-Film Transistors.....	25
2.2.1 Experimental Procedure and Results.....	25
2.2.2 Comparison of Different Layout Methods.....	30
2.3 Devices Fabrication of the Low-Temperature Polycrystalline-Silicon Thin Film Transistors with Multi-Channel Structure.....	39
2.3.1 Experimental Procedure.....	39
2.3.2 Measured Results and Discussion.....	42
2.4 Discussions of the Improved Uniformity Mechanisms between the Conventional and Multi-channel Structures.....	51
2.5 Summary.....	55
Chapter 3 Evaluated Results of Conventional Pixel Circuit, Other Compensation Circuits and Proposed Pixel Circuits for Active Matrix Organic Light Emitting Diodes (AMOLEDs).....	56
3.1 Introduction.....	56
3.2 Simulation Results of Dimensional Effects on Transistors and Storage	

Capacitor in Conventional Pixel Circuit.....	59
3.2.1 The Effect of Switching TFT.....	61
3.2.2 The Effect of Driving TFT.....	62
3.2.3 The Effect of Storage Capacitor.....	63
3.2.4 The Effect of Transistor Slicing Layout.....	64
3.3 Digital Driving Circuits.....	66
3.3.1 Area Ratio Gray Scale Method (ARG).....	66
3.3.2 Time Ratio Gray Scale Method (TRG).....	67
3.4 Simulation Results of Analog Driving Circuits.....	68
3.4.1 Voltage Programming Circuits.....	69
3.4.1.1 Self-Compensation Method.....	69
3.4.1.2 Matching TFTs Method.....	70
3.4.1.3 Resistance or Active Load Method.....	71
3.4.1.4 Diode Connection Method.....	72
3.4.1.5 AC Driving Method.....	74
3.4.2 Current Programming Circuits.....	75
3.4.2.1 Current Copy Method.....	75
3.4.2.2 Current Mirror Method.....	76
3.4.3 Novel Driving Circuits.....	77
3.5 Proposed Pixel Circuit Design.....	81
3.5.1 Compensation Method Using Diode Connection Concept.....	81
3.5.2 Simulation Results and Discussion.....	82
3.6 Modified Pixel Circuit Design.....	88
3.7 Comparison between the Proposed Pixel Circuits and Other Pixel Circuits Design.....	95

3.8 Several-Frames Issue of the Proposed Pixel Circuit.....	96
3.9 Summary.....	102

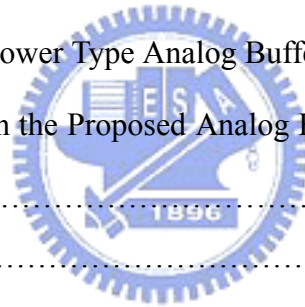
Chapter 4 Experimental Results of the Conventional and Proposed Pixel Circuits for Driving Organic Light Emitting Diodes Using Low-Temperature Polycrystalline Silicon Thin Film Transistors.....104

4.1 Introduction.....	104
4.2 Experimental Procedures and the Setup of Measurement System.....	106
4.3 Experimental Results of Dimensional Effects on Transistors and Storage Capacitor in Conventional Pixel Circuit.....	111
4.3.1 The Effect of Switching TFT.....	111
4.3.2 The Effect of Driving TFT.....	112
4.3.3 The Effect of Storage Capacitor.....	113
4.3.4 The Effect of Transistor Slicing Layout.....	114
4.4 Experimental Results of Proposed Pixel Circuit Design.....	117
4.5 Summary.....	119

Chapter 5 Evaluated Results and Comparisons of Source Follower Type, Operational Amplifier Type, and Proposed Analog Buffer Circuits.....120

5.1 Introduction.....	120
5.2 Considerations for Designing of LTPS-TFTs Analog Buffer Circuits.....	122
5.3 Simulation Results of Operational Amplifier Type (Op-amp-type) Analog	

Buffer.....	123
5.3.1 Typical Op-amp-type Analog Buffer.....	123
5.3.2 Bias Circuit Op-amp-type Analog Buffer.....	125
5.3.3 Differential Pair Op-amp-type Analog Buffer.....	126
5.4 Simulation Results of Source Follower Type Analog Buffer.....	128
5.4.1 Conventional Source Follower Type Analog Buffer.....	128
5.4.2 Self-Compensation Method.....	130
5.4.3 Matching TFTs Method.....	135
5.5 Issues of Conventional Source Follower Type Analog Buffer.....	136
5.5.1 Unsaturated Output Voltage Phenomenon of the Analog Buffer.....	138
5.5.2 Output Voltage Distributed Phenomenon of the Analog Buffer.....	139
5.6 Proposed Source Follower Type Analog Buffer.....	140
5.7 Comparisons between the Proposed Analog Buffer Circuit and Other Analog Buffer Circuits Design.....	144
5.8 Summary.....	146



Chapter 6 Experimental Results of the Conventional and Proposed Source Follower Type Analog Buffer Circuits148

6.1 Introduction.....	148
6.2 Measured Results of the Effect of Transistor Slicing Layout Method on Conventional Analog Buffer Circuit.....	149
6.3 Proposed Source Follower Type Analog Buffer Fabrication and Measured Results.....	153
6.4 Bias Voltage Effects on Offset Voltage.....	156
6.5 Summary.....	161

Chapter 7 Summary and Conclusions.....163

Chapter 8 Future Prospects.....167

References.....170

Publication Lists

Vita



Table Lists

Chapter 2

Table 2-1 Comparisons of electrical characteristics between single channel structure and multi-channel in $W=10\mu\text{m}$ and $W=200\mu\text{m}$

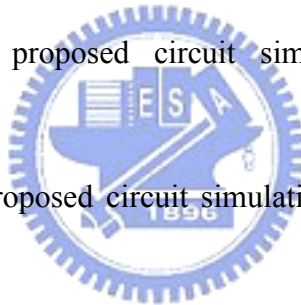
Chapter 3

Table 3-1 Timing period and device parameters of proposed pixel circuit simulation.

Table 3-2 Parameters of proposed circuit simulation with changed timing period.

Table 3-3 Parameters of proposed circuit simulation with changed device dimension.

Table 3-4 Parameters of proposed circuit simulation with changed timing period and device dimension.



Chapter 5

Table 5-1 The output settling time of the proposed analog buffer with input voltage ranges from 1V to 5V.

Table 5-2 Timing period and device parameters of proposed analog buffer circuit simulation.

Table 5-3 Comparisons of the proposed analog buffer and others buffer circuits.

Figure Captions

Chapter 2

Fig. 2-1. (a) The differential pair circuit, (b) Parallel arrangement layout method corresponding to excimer laser scanning direction of matching TFTs

Fig. 2-2. Normalized output characteristics (i.e. W/L ratio=1) for non-passivated p-channel matching TFTs with (a) $W/L = 2\mu\text{m}/2\mu\text{m}$, (b) $3\mu\text{m}/3\mu\text{m}$, (c) $6\mu\text{m}/6\mu\text{m}$, and (d) $12\mu\text{m}/12\mu\text{m}$. The small dimension exhibits larger output current and more serious kink effect.

Fig. 2-3. Perpendicular arrangement layout method corresponding to excimer laser scanning direction of matching TFTs.

Fig. 2-4. Interdigitated arrangement layout method corresponding to excimer laser scanning direction of matching TFTs.

Fig. 2-5. Threshold voltage difference between different layout methods of matching TFTs with different channel widths and channel lengths (a) parallel arrangement, (b) parallel arrangement in magnified scale, (c) perpendicular arrangement, and (d) interdigitated arrangement.

Fig. 2-6. Field-effect mobility difference between different layout methods of matching TFTs with different channel widths and channel lengths (a) parallel arrangement, (b) perpendicular arrangement, and (c) interdigitated arrangement.

Fig. 2-7. (a) Threshold voltage and (b) Field-effect mobility measured from p-channel LTPS TFTs with different active areas. The worse mismatching factor is

around 0.2 (20% mismatch) in device characteristics, and the usual mismatching factor is around 0.05 (5% mismatch) in device characteristics.

Fig. 2-8. The comparison of layout and circuit configuration between conventional single channel TFTs and multi-channel TFTs.

Fig. 2-9. The process procedure of fabricating ELC LTPS TFTs.

Fig. 2-10. Output characteristics of thirty LTPS TFTs at $V_{gs}=10V$ in (a) single channel devices, (b) multi-channel devices with five stripes, and (c) multi-channel devices with ten stripes.

Fig. 2-11. Transfer characteristics of thirty LTPS TFTs at $V_{ds} = 0.1 V$ in (a) single channel devices, (b) multi-channel devices with five stripes, and (c) multi-channel devices with ten stripes.

Fig. 2-12. The comparison of cumulative distributions for the threshold voltage from twenty-five n type LTPS-TFTs ($W/L=10\mu m/5\mu m$) in single channel structure and multi-channel structure.

Fig. 2-13. The comparison of cumulative distributions for the sub-threshold swing from twenty-five n type LTPS-TFTs ($W/L=10\mu m/5\mu m$) in single channel structure and multi-channel structure.

Fig. 2-14. The comparison of cumulative distributions for the transconductance from twenty-five n type LTPS-TFTs ($W/L=10\mu m/5\mu m$) in single channel structure and multi-channel structure.

Fig. 2-15. The comparison of cumulative distributions for the threshold voltage from twenty-five n type LTPS-TFTs ($W/L=200\mu m/5\mu m$) in single channel structure and multi-channel structure.

Fig. 2-16. The comparison of cumulative distributions for the sub-threshold swing from twenty-five n type LTPS-TFTs ($W/L=200\mu m/5\mu m$) in single channel

structure and multi-channel structure.

Fig. 2-17. The comparison of cumulative distributions for the transconductance from twenty-five n type LTPS-TFTs ($W/L=200\mu\text{m}/5\mu\text{m}$) in single channel structure and multi-channel structure.

Fig. 2-18. Cross-section view of the multi-channel structure.

Fig. 2-19. (a) Probable distribution of relative location between devices and grains in single channel structure. (b) Probable distribution of relative location between devices and grains in multi-channel structure.

Chapter 3

Fig. 3-1. Typical N-type LTPS TFT pixel circuit for AMOLED.

Fig. 3-2. The measured and simulation result of OLED's current versus bias voltage characteristics.

Fig. 3-3. The measured and simulation results of n type LTPS TFT's transfer characteristics.

Fig. 3-4. The simulation results are compared with the varied switching TFT dimensions.

Fig. 3-5. The simulation results are compared with the varied driving TFT dimensions.

Fig. 3-6. The simulated voltages stored in the capacitors with varied capacitances when the input data voltage= 5V.

Fig. 3-7. Comparison of the slicing method effect in simulation and measured results of OLED anode voltages versus input data voltage ranges 1V to 6V.

Fig. 3-8. Comparison of the slicing method effect in simulation and measured

results of non-uniformity versus input data voltage ranges 1V to 6V.

- Fig. 3-9. Pixel circuitry of area ratio gray scale method.
- Fig. 3-10. Timing diagram of time ratio gray scale method.
- Fig. 3-11. An example of self-compensation pixel circuit and its timing diagram.
- Fig. 3-12. An example of matching transistors pixel circuit and its timing diagram.
- Fig. 3-13. An example of active load method pixel circuit.
- Fig. 3-14. (a) Diode connected transistors for n channel and p channel transistors. (b)
Example of diode-connected method pixel circuit.
- Fig. 3-15. An example of AC driving pixel circuit.
- Fig. 3-16. Current copy pixel circuit and its timing diagram.
- Fig. 3-17. Current mirror pixel circuit and its timing diagram.
- Fig. 3-18. Polarity balanced driving method and driving sequence.
- Fig. 3-19. Clamped inverter driving method and timing chart.
- Fig. 3-20. Time division control driving method and timing diagram.
- Fig. 3-21. Examples of compensation by diode connection in the n type TFT circuit
and p type TFT circuit.
- Fig. 3-22. Transient response of the conventional 2T1C pixel circuit.
- Fig. 3-23. Proposed circuit schematic and driving signals of voltage compensation
circuit for AMOLED.
- Fig. 3-24. Transient response of the proposed pixel circuit.
- Fig. 3-25. An example of driving scheme for the stored data voltage in the capacitor
with varied threshold voltages of TFTs.
- Fig. 3-26. Thirty times Monte Carlo simulation results of conventional pixel circuit.
- Fig. 3-27. Thirty times Monte Carlo simulation results of proposed pixel circuit.
- Fig. 3-28. The measured and simulated transfer characteristics of p channel TFT.
- Fig. 3-29. Modified pixel circuit schematic and the timing diagram of control

signals.

- Fig. 3-30. Transient response of the modified pixel circuit.
- Fig. 3-31. An example of driving scheme for the stored data voltage in the capacitor with varied threshold voltages of TFTs in the modified pixel circuit.
- Fig. 3-32. Comparison of the output current non-uniformity.
- Fig. 3-33. Simulation results showing the range of current flowing through the OLED at different V_{data} and threshold voltage variation ($\Delta V_{th} = -0.33V$, $0V$, and $+0.33V$).
- Fig. 3-34. The error rate of output current in our proposed pixel circuit.
- Fig. 3-35. Power reduction of the modified circuit design compared with the first one.
- Fig. 3-36. Non-uniformity of the output current for $\pm 0.33V$ threshold voltage fluctuations.
- Fig. 3-37. Power dissipation of the circuit designs for different input data voltages.
- Fig. 3-38. Variations of the proposed circuit simulation with data voltage = 3, 3.5, 1, 2V.
- Fig. 3-39. Variations of proposed circuit simulation with data voltage = 0.5, 5, 0, 2V.
- Fig. 3-40. Variations of proposed circuit simulation with changed timing period.
- Fig. 3-41. Variations of the proposed circuit simulation with changed device dimension.
- Fig. 3-42. Variations of proposed circuit simulation with changed timing period and device dimension.

Chapter 4

- Fig. 4-1. Cumulative distributions of the (a) threshold voltage, (b) field-effect mobility, (c) sub-threshold swing from thirty n-channel LTPS TFTs fabricated on the same glass substrate.
- Fig. 4-2. Optical micrograph of conventional pixel circuit and its applied signals.
- Fig. 4-3. Optical micrograph of the proposed pixel circuit.
- Fig. 4-4. Measurement system for testing pixels.
- Fig. 4-5. The simulation and experimental results are compared with the varied switching TFT dimensions.
- Fig. 4-6. The simulation and experimental results are compared with the varied driving TFT dimensions.
- Fig. 4-7. The measured voltages stored in the capacitors with varied capacitances when the input data voltage= 5V.
- Fig. 4-8. Comparison of the slicing method effect in simulation and measured results of OLED anode voltages versus input data voltage ranges 1V to 6V.
- Fig. 4-9. Comparison of the slicing method effect in simulation and measured results of non-uniformity versus input data voltage ranges 1V to 6V.
- Fig. 4-10. The measured results the proposed pixel circuit compared to conventional pixel circuit with different data voltages.
- Fig. 4-11. The measured and simulation results of non-uniformity compared with conventional 2T1C pixel circuit.

Chapter 5

- Fig. 5-1. Block diagram of AMLCD panel.
- Fig. 5-2. Functional blocks of data driver circuits in AMLCD panel.

- Fig. 5-3. Circuit configuration of the typical operational amplifier.
- Fig. 5-4. Monte Carlo simulation results of the typical op-amp-type analog buffer with varied input voltage from 1V to 6V.
- Fig. 5-5. Yiu's bias circuit compensated operational amplifier type analog buffer.
- Fig. 5-6. Monte Carlo simulation results of the Yiu's operational amplifier type analog buffer with varied input voltages.
- Fig. 5-7. Itou's differential amplifier compensated operational amplifier type analog buffer.
- Fig. 5-8. Monte Carlo simulation results of the Itou's operational amplifier type analog buffer with varied input voltages.
- Fig. 5-9. Schematic of conventional source follower type analog buffer.
- Fig. 5-10. Monte Carlo simulation results of the output offset voltage variations in conventional source follower type analog buffer.
- Fig. 5-11. Schematic and timing diagrams of Chung's push-pull type analog buffer.
- Fig. 5-12. Monte Carlo simulation results of the offset voltage variations of Chung's push-pull type analog buffer.
- Fig. 5-13. Circuit configuration and timing diagrams of double-offset-canceling analog buffer.
- Fig. 5-14. Monte Carlo simulation results of the offset voltage variations of double-offset-canceling analog buffer.
- Fig. 5-15. Schematic and timing diagrams of Yoo's analog buffer.
- Fig. 5-16. Monte Carlo simulation results of the offset voltage variations of Yoo's analog buffer.
- Fig. 5-17. Schematic and timing diagrams of matching TFTs type analog buffer.
- Fig. 5-18. Monte Carlo simulation results of the offset voltage variations of matching TFTs type analog buffer.

Fig. 5-19. Conventional source follower and its output waveform simulation results.

Fig. 5-20. Schematic of conventional source follower with an active load and its output waveform simulation results.

Fig. 5-21. Offset voltage comparison of conventional source follower and source follower with an active load in various charging time.

Fig. 5-22. Twenty times of Monte Carlo simulation results of the conventional source follower with an active load when input voltage 2V to 4V.

Fig. 5-23. The proposed analog buffer and its timing diagram of signal lines.

Fig. 5-24. Twenty times of Monte Carlo simulation results of the proposed analog buffer when input voltage 2V to 4V.

Chapter 6



Fig. 6-1. Schematic configuration of the conventional analog buffer with the signal channel (left) and multi-channel (right) driving TFT.

Fig. 6-2. Ten sets measured results of the offset voltage ($V_{in}-V_{out}$) variations versus varied input voltages employed single channel structures.

Fig. 6-3. Ten sets measured results of the offset voltage ($V_{in}-V_{out}$) variations versus varied input voltages employed multi-channel structures.

Fig. 6-4. Comparison of the measured output offset voltage variations between the single channel and multi-channel structure.

Fig. 6-5. The optical micrograph of the proposed of fabricated circuit.

Fig. 6-6. Comparison of the measured offset voltage versus input voltage curve of the conventional and proposed analog buffers.

Fig. 6-7. Variations of eight buffer circuits between the offset voltage versus input

voltage of the conventional and proposed analog buffers.

Fig. 6-8. Simulation results of the output offset voltage and the power dissipation for the proposed analog buffer with different bias voltage.

Fig. 6-9. Comparison of the offset voltage versus bias voltage curve of the simulation and measured results when input voltage 3V.

Fig. 6-10. Comparison of the offset voltage versus bias voltage curve of the simulation and measured results when input voltage 2V.

